Amino Acids (2018) 50:1583–1594
https://doi.org/10.1007/s00726-018-2635-2

ORIGINAL ARTICLE

Allosteric inhibition site of transglutaminase 2 is unveiled in the N terminus

Nayeon Kim[1] · Joon Hee Kang[1] · Won-Kyu Lee[2] · Seul-Gi Kim[1] · Jae-Seon Lee[1] · Seon-Hyeong Lee[1] · Jong Bae Park[3] · Kyung-Hee Kim[4] · Young-Dae Gong[5] · Kwang Yeon Hwang[6] · Soo-Youl Kim[1]

Received: 17 May 2018 / Accepted: 9 August 2018 / Published online: 14 August 2018

Abstract

Previously we have demonstrated transglutaminase 2 (TGase 2) inhibition abrogated renal cell carcinoma (RCC) using GK921 (3-(phenylethynyl)-2-(2-(pyridin-2-yl)ethoxy)pyrido[3,2-b]pyrazine), although the mechanism of TGase 2 inhibition remains unsolved. Recently, we found that the increase of TGase 2 expression is required for p53 depletion in RCC by transporting the TGase 2 (1–139 a.a)–p53 complex to the autophagosome, through TGase 2 (472–687 a.a) binding p62. In this study, mass analysis revealed that GK921 bound to the N terminus of TGase 2 (81–116 a.a), which stabilized p53 by blocking TGase 2 binding. This suggests that RCC survival can be stopped by p53-induced cell death through blocking the p53–TGase 2 complex formation using GK921. Although GK921 does not bind to the active site of TGase 2, GK921 binding to the N terminus of TGase 2 also inactivated TGase 2 activity through acceleration of non-covalent self-polymerization of TGase 2 via conformational change. This suggests that TGase 2 has an allosteric binding site (81–116 a.a) which changes the conformation of TGase 2 enough to accelerate inactivation through self-polymer formation.

Keywords Transglutaminase 2 · p53 · Allosteric binding site · GK921

Introduction

Transglutaminase 2 (TGase 2) catalyzes intra- and intermolecular Nε-(γ-glutamyl)-lysine crosslinks (E.C. 2.3.2.13) between the γ-carboxamide groups of peptide-bound glutamine residues, which act as acyl donors, and the γ-amino groups of protein- and peptide-bound lysine residues, which act as acceptors (Folk 1983). Recently, TGase 2 has been identified as a therapeutic target (Kang et al. 2016; Ku et al. 2013, 2014) as well as a significant clinicopathologic marker in human clear cell renal cell carcinoma (RCC) (Park et al. 2015). RCC shows highly increased expression of TGase 2 regardless of mutations, while low expression has been detected in the normal kidney epithelial cell. The high expression of TGase 2 is explained with down-regulation of mir-1285 that is responsible for suppression of TGase 2 in RCC (Hidaka et al. 2012). We found that TGase 2 knockdown or TGase 2 inhibition stabilized p53 in RCC, which induced p53-mediated apoptosis because there is less than 4% mutation of p53 in RCC (Kang et al. 2016). A recent report showed that TGase 2 is also a key molecular switch of necrosis-induced mesenchymal trans-differentiation by regulating master transcription factors such as C/EBPβ, TAZ,

Handling Editor: S. Beninati.

Nayeon Kim and Joon Hee Kang contributed equally to the manuscript.

Electronic supplementary material The online version of this article (https://doi.org/10.1007/s00726-018-2635-2) contains supplementary material, which is available to authorized users.

✉ Soo-Youl Kim
kimsooyoul@gmail.com

[1] Tumor Microenvironment Branch, Division of Cancer Biology, Research Institute, National Cancer Center, Goyang 10408, Republic of Korea

[2] New Drug Development Center, Osong Medical Innovation Foundation, Cheongju, Chungbuk 28160, Republic of Korea

[3] Department of System Cancer Science, Graduate School of Cancer Science and Policy, National Cancer Center, Goyang 10408, Republic of Korea

[4] Omics Core Lab, Research Institute, National Cancer Center, Goyang 10408, Republic of Korea

[5] Department of Chemistry, College of Science, Dongguk University, Seoul 04620, Republic of Korea

[6] Institute of Life Science and Natural Resources, Korea University, Seoul 02841, Republic of Korea

and STAT3 through GADD153 depletion in glioblastoma, which is correlated with recurrent mesenchymal patients and inversely correlated with patient prognosis (Yin et al. 2017). Currently, despite the effort of many groups, no small molecule TGase 2 inhibitors are available for clinical trials.

Previously, we have introduced a pyrido[2,3-*b*]pyrazine derivative of TGase 2 inhibitor, GK921, 3-(phenylethynyl)-2-(2-(pyridin-2-yl)ethoxy)pyrido[2,3-*b*]pyrazine by inhibitory activity screening (Ku et al. 2014). GK921 demonstrated RCC regression successfully through p53 stabilization with TGase 2 inhibition although the detail inhibitory mechanism remains to be answered (Ku et al. 2014). TGase 2 inhibition using GK921 also blocked mesenchymal trans-differentiation and showed significant therapeutic effect in the mouse glioblastoma model (Yin et al. 2017). Therefore, understanding the mechanism of GK921 inhibiting TGase 2 may lead to the development of a new therapeutic approach.

Materials and methods

TGase 2 activity assay

Succinylated casein obtained from Calbiochem (Cat. No. 573,464) was dissolved as 2% in 0.1 M Tris–acetate buffer (pH 8.0) containing 10 mM $CaCl_2$, 0.15 M NaCl, 1.0 mM EDTA (5 mM DTT added just before use). Putrescine dihydrochloride [1,4-^{14}C] purchased from American Radiolabeled Chemicals, Inc. (Cat. no. ARC-245). 250 µCi of putrescine dihydrochloride dissolved in 122.5 ml DW, which gives 2 µCi/ml. TGase 2 purified from guinea pig liver for activity assay was obtained from Zedira (T006, Darmstadt, Germany). This was dissolved as 600 ng/µl in 50 mM Tris–HCl buffer (pH 7.5) containing 1 mM EDTA. 1X TEN buffer composed of 100 mM Tris–acetate buffer (pH 8.0), 1 mM EDTA, and 150 mM NaCl. Glass microfiber filters were purchased from Whatman GF/A (Cat. no. 1820-025).

In each assay vial, 48.58 µl of TEN buffer and 0.42 µl of 600 ng/µl gpTG2 were added. Then, 1 µl of four different concentrations of GK921 (0.1 mM, 0.5 mM, 1 mM, 5 mM) was added to the assay vial. The assay vials were pre-incubated at RT for 30 min. 140 µl of 2% succinylated casein (5 mM DTT) and 10 µl of 2 µCi/ml putrescine were added to each assay vial and incubated in 37 °C thermomixer for 30 min. Reaction was stopped by adding 2 ml of cold 5% TCA. The assay vials were fixed in 4 °C for at least 1 h. Assay mix was filtered onto glass fiber filter paper disc and washed with cold 5% TCA. Filter was placed into counting vial and 4 mL of scintillation cocktail solution was added. Counting vial was vortexed for 5 s and placed on shaker for 30 min before counting.

Antibodies and reagents

GK921 is synthesized by Y.-D. Gong' Laboratory. The following antibodies were used for TGase 2 (Cat. #MS-300-P0, Thermo Scientific, IL, USA, 1:1000), HA-probe (Cat. #sc-7392, Santa Cruz Biotechnology, TX, USA, 1:1000), p53 (Cat. #sc-126, Santa Cruz Biotechnology, TX, USA, 1:500), FLAG (cat. #F7425, Merck, USA, 1:1000), and human p53 recombinant protein (Cat. #BML-FW9370-0050, Enzo, NY, USA). To identify the TG2 binding site of GK921, the HA-pcDNA3.1/TGase 2 quadruple point mutant type plasmid (Q95A, Q96A, Q103A, R116A) was constructed based on TGase2 wild-type plasmids which was previously described (Ku et al. 2013). The p3xFLAG p53 plasmid was constructed based on the p3xFLAG vector. The sequences of primer pairs used in the present study are listed in supplemental Table 1. All constructs were confirmed by DNA sequencing.

Cell culture

A498, ACHN, RXF 393, TK10, CAKI-1 and UO31 cells were obtained from the National Cancer Institute (MTA: 2702-09). Cells were cultured in complete RPMI 1640 medium (Hyclone, UT, USA) containing 10% fetal bovine serum (Hyclone, UT, USA) in an atmosphere of 5% CO_2 and 100% humidity at 37 °C. HEK293 cells were cultured in Dulbecco's modified Eagle's medium (Hyclone, UT, USA) containing 10% fetal bovine serum.

Western blotting

Whole cell lysate was prepared using RIPA buffer containing 50 mM Tris–HCl, pH 8.0, with 150 mM sodium chloride, 1.0% Igepal CA-630 (NP-40), 0.5% sodium deoxycholate, 0.1% sodium dodecyl sulfate, protease inhibitor cocktail, and phosphatase inhibitor cocktail. Protein assays were carried out to normalize the proteins using a BCA protein assay (Thermo Scientific, IL, USA). Proteins were resolved by SDS-PAGE and were transferred to polyvinylidene difluoride (PVDF) membrane (Merck Millipore, MA, USA). Membranes were blocked in 5% BSA for 1 h at R.T. and incubated with indicated antibodies overnight at 4 °C. Membranes were washed in TBS-T for 1 h at R.T. and incubated with horseradish peroxidase-conjugated secondary antibody for 1 h at R.T. Finally, membranes were washed in TBS-T for 1 h at R.T. and developed using enhanced chemiluminescence.

SRB assay for anti-proliferative activity

GK921 was tested for anti-proliferative activity using the established method of sulforhodamine B (SRB). Cells (100 µl containing 5000–40,000 cells/well, depending on

the doubling time of the individual cell lines) were incubated in 96-well microtiter plates. After 24 h, GK921 was added (100 µl) to each well and the cultures were incubated for 48 h at 37 °C. The cells were then fixed in 50% trichloroacetic acid (50 µl per well). The plate was incubated for an hour at 4 °C. The liquid was removed from the plate, which was then rinsed five times with water and allowed to dry at room temperature (RT) for approximately 12–24 h. The fixed cells were stained with 100 µl SRB for 5 min at RT. After staining, the plate was washed three times with 1% glacial acetic acid and dried at RT for approximately 12–24 h. The SRB stain was then solubilized in 10 mM Trizma base and the absorbance was read at 515 nm. The effect of the drugs was expressed as GI_{50} (50% growth inhibition), TGI (total growth inhibition), or LC_{50} (lethal concentration).

Analysis of GK921 binding site in TGase 2 by mass spectroscopy

Sample preparation—1 mM GK921 was incubated with 0.5 milliunit of purified recombinant human TGase 2 (T002, Zedira, Darmstadt, Germany) in a reaction mixture containing 100 mM Tris, pH 7.5, 100 mM NaCl, 1 mM EDTA and 2 mM $MgCl_2$ with or without each of the indicated. After 30 min at 37 °C, the reactants were analyzed separately by LC–MS/MS.

In-solution tryptic digestion—0.4 mg of protein samples was used for in-solution tryptic digestion, according to the manufacturer's instructions using filter-assisted sample preparation (FASP) protein digestion kit (Expedeon Inc., CA, USA). Briefly, the sample was mixed with 200 µl of urea sample solution in the spin filter and centrifuged at 14,000×*g* for 15 min. Proteins on the spin filter were alkylated by iodoacetamide (IAA). The alkylated proteins in the filter were washed, and 50 mM NH4HCO3 was added to the spin filter. Trypsin digestion was conducted at 37 °C overnight using MS-grade trypsin (Thermo Fisher Scientific, Rockford, IL, USA). After incubation, peptides were extracted by adding 50 µl of 0.5 M sodium chloride solution and centrifuging at 14,000×g for 10 min. Digested peptides were cleaned up using C18 Zip Tip (Millipore, MA, USA), evaporated using vacuum concentrator, and resuspended in 20 µl 0.1% formic acid for LC–MS analysis.

LC–MS/MS analysis and database search—The tryptic-digested peptides were analyzed by Q Exactive™ hybrid quadrupole Orbitrap mass spectrometer (Thermo Fisher Scientific, MA, USA) coupled with an Ultimate 3000 RSLCnano system (Thermo Fisher Scientific, MA, USA). The tryptic peptides were loaded onto trap column (100 µm × 2 cm) packed with Acclaim PepMap100 C18 resin, in which loaded peptides were eluted with a linear gradient from 5 to 35% solvent B (0.1% formic acid in ACN) for 30 min at a flow rate 300 nL/min. The eluted peptides, separated by the analytical column (75 µm × 15 cm), were sprayed into nano-ESI source with an electrospray voltage of 2.4 kV. The Q Exactive Orbitrap mass analyzer was operated in a top 10 data-dependent method. Full MS scans were acquired over the range m/z 300–2000 with mass resolution of 70,000 (at m/z 200). The AGC target value was 1.00E + 06. The ten most intense peaks with charge state ≥ 2 were fragmented in the higher energy collisional dissociation (HCD) collision cell with normalized collision energy of 25%, and tandem mass spectra were acquired in the Orbitrap mass analyzer with a mass resolution of 17,500 at m/z 200.

Database searching of all raw data files was performed in Proteome Discoverer 1.4 software (Thermo Scientific, IL, USA). MASCOT 2.3.2 and SEQUEST were used for database searching against Uniprot database. Database searching against the corresponding reversed database was also performed to evaluate the false discovery rate (FDR) of peptide identification. The database searching parameters included up to two missed cleavages allowed for full tryptic digestion, precursor ion mass tolerance 10 ppm, fragment ion mass tolerance 0.02 Da, fixed modification for carbamidomethyl cysteine and variable modifications for methionine oxidation and N/Q deamination. We obtained an FDR of less than 1% on the peptide level and filtered with the high peptide confidence.

Native gel electrophoresis

GK921 was incubated for 30 min at 37 °C in a buffer of 100 mM Tris–HCl, pH 8.0, 100 mM NaCl, 1 mM EDTA, 2 mM $MgCl_2$, 10 mM DTT with purified human recombinant TGase 2 (0.5 µg) (T002, Darmstadt, Germany), LDH (0.5 µg) and fibrinogen (0.5 µg). Laemmli native buffer (without SDS and reducing agent) was added and 0.2 µg of protein (TGase 2, LDH and Fibrinogen) was loaded onto 10% native gel using Tris/glycine as the running buffer at 4 °C. Following electrophoresis, the gel was stained with Coomassie dye and imaged using a flatbed scanner.

Gel electrophoresis

The samples were the same ones used in native gel electrophoresis. Laemmli buffer was added and 0.2 µg of protein (TGase 2, LDH and fibrinogen) was loaded onto 10% SDS gel using Tris/glycine as the running buffer. After electrophoresis, the gel was stained with Coomassie dye and imaged using a flatbed scanner.

Immunoprecipitation

To determine GK921 binding to TGase 2 in vitro, TGase 2 (100 ng) was incubated with GK921 (0, 0.5, 1 µM) for 10 min

on 4 °C in 30 µl of reaction buffer containing 0.1 M Tris–Cl, 1 mM EDTA, 2 mM $MgCl_2$, and 0.1 M NaCl, pH 8.0. Then, p53 (100 ng) was added to make a total of 40 µl reaction mixture, which reacted for 30 min on 37 °C. In binding test using cell line, HEK293 cells were transfected with HA-TGase 2 (2 µg) and 3xFLAG-p53 (1 µg). After 24-h transfection, HEK293 and ACHN cells were treated with 0, 0.5, 1.0 and 2.0 µM of GK921 for 24 h. Cell lysate was prepared using RIPA buffer for immunoprecipitation. Each lysate was mixed with antibodies (1 µg/ml) of p53 and HA at 4 °C overnight in immunoprecipitation buffer containing 50 mM Tris–Cl, 150 mM NaCl, 1 mM EDTA, 0.5% Triton X-100, pH 7.4 and reacted with 10 µl of protein A/G beads UltraLink Resin (50:50 resin: buffer slurry condition) (Peirce, #35133) for 2 h on RT for precipitation. After reaction and centrifugation at 3000 rpm for 3 min, the immunoprecipitated samples were washed with 500 µl of immunoprecipitation buffer by tapping and centrifuged. The washing was repeated five times before western blotting.

Isothermal titration calorimetry (ITC) assay: thioflavin T assay for the identification of GK921 binding

GK921 to be tested was dissolved at 1000, 500, 250, 125 and 62.5 µM in 100% DMSO. The final DMSO concentration was 1%. The ThT signal was quantified by averaging the fluorescence emission at 500 nm over 10 s when excited at 442 nm, using the TRIAD multimode detector TRIAD LT (Dynex Technologies, Chantilly, VA, USA) plate reader in 96-well black plates.

Molecular docking

Molecular docking experiments were performed using Discovery studio 2017, program version 4.5. 2Q3Z; a crystal structure of open conformation human TGase 2 was used as a protein molecule. A binding site was created with a radius of 10 Å around the ligand present in the N-terminal domain of TGase 2 by MS analysis results. GK921 and Thioflavin T were docked into the created binding site. All options were kept default during docking experiments. The final docking model was selected based on the binding mode and molecular interactions observed at the active site. Also, the calculation of non-covalent interaction and the drawing of 2D interaction diagram were made by Discovery studio 2017.

Results

GK921 inhibited TGase 2 activity in vitro

TGase 2 inhibitory effect of GK921 has been reported followed by development of GK13 quinoxaline derivative based on in vitro inhibition assay of recombinant human TGase 2 activity (IC50: 8.93 µM) as well as in vitro competition assay of p53 binding to TGase 2 (Ku et al. 2014). However, we did not find evidence how GK921 inhibits TGase 2 because GK921 does not have a warhead of attacking cysteine active site of TGase 2. The best answer is the co-crystallization of TGase 2 with GK921, but it is unable to obtain the suitable experimental results in a complexed situation due to folded or unfolded form of TGase 2 (Pinkas et al. 2007) as well as due to monomeric or dimeric formation by temperature dependence (Kim et al. 2017). GK921 (Fig. 1a) showed TGase 2 inhibitory activity as 8.93 µM of IC_{50} under a modified assay condition, which concurred with a previous report (Ku et al. 2014) (Supple Fig. 1a). Isothermal titration calorimetry (ITC) analysis also showed that GK921 binds TGase 2 in a dose-dependent manner (Fig. 1b). Cell proliferating assay using sulforhodamine B (SRB) showed that GK921 induced cell growth inhibition in RCC cells (Fig. 1c). All those six RCC cell lines showed highly increased expression of TGase 2 regardless of mutations (Ku et al. 2013).

GK921 binding at the N terminus of TGase 2

To identify the binding site of GK921 in TGase 2, fluorescence experiment and mass analysis approach were adopted (Fig. 1b and Supple Fig. 2). Originally, this fluorescent material is frequently used for the observation of aggregation of amyloid beta. It observes the change in fluorescence that occurs when the ThT binds to the beta structure formed during aggregation. When GK921 was treated with ThT fluorescent probe bound to TGase 2 using the characteristics of the ThT, it was predicted that fluorescence would change due to the breakdown of ThT bound to the N-terminal beta structure of TGase 2. The concentration-dependent change was also observed as expected (Fig. 1b). To identify blocking region of TGase 2 by GK921, mass analysis was performed using proteolytic digestion with two different peptidases after incubation of GK921 with recombinant human TGase 2 in vitro. We have identified that the N terminus of TGase 2 was the only overlapped blocking region from the results by digestion with two different peptidases (Fig. 2a, Supple Fig. 2). Mass analysis was performed with a mixture of TGase 2 and GK921 after 30-min incubation at 37 °C.

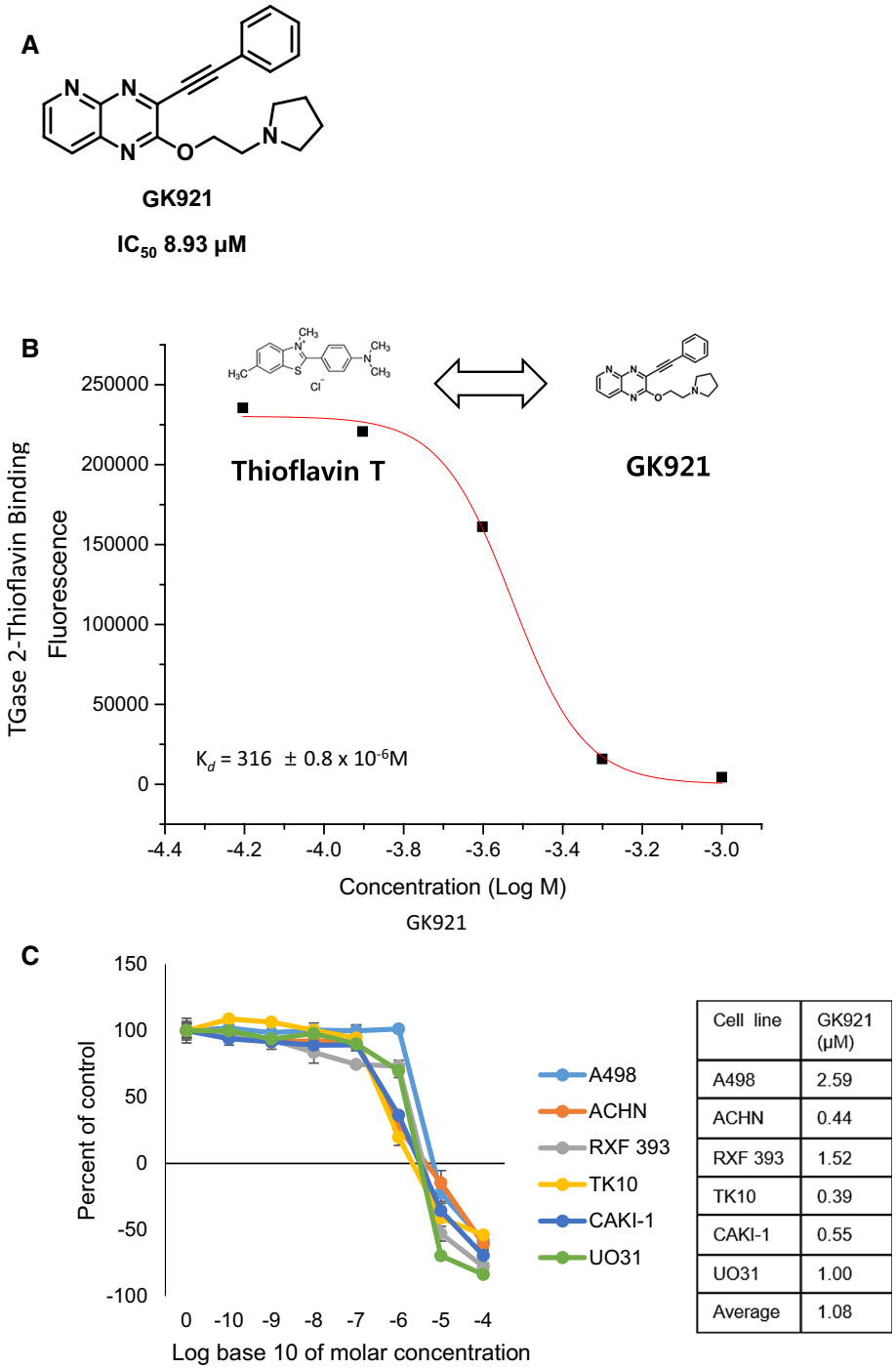

Cell line	GK921 (μM)
A498	2.59
ACHN	0.44
RXF 393	1.52
TK10	0.39
CAKI-1	0.55
UO31	1.00
Average	1.08

Fig. 1 GK921 as a TGase 2 inhibitor. **a** Chemical structure of GK921. The IC_{50} value of GK921 against purified guinea pig TGase 2 is 8.93 μM (Supple Fig. 1a). **b** GK921 binding study using the Thioflavin T. The calculated K_d value of GK921 against TGase 2 is 316 ± 0.8 μM. **c** The cytotoxicity of GK921 was analyzed by SRB assay on human renal cell carcinoma cell lines. Average GI_{50} was 1.08 μM. Data are representative of the mean and standard deviation of three independent experiments

The covered mass area by mass identification was marked in green (strong) and red (weak) while unidentified area was marked in black (Supple Fig. 2). The mass analysis of TGase 2 with GK921 clearly reduced identification of the N-terminal region at 95–97 a.a by glu-c digestion compared to the control (Fig. 2a, Supple Fig. 2a, c) or at 81–116 a.a by trypsin (Fig. 2a, Supple Fig. 2b, d). This implies that the binding region of GK921 is located at 81–116 a.a (Fig. 2a). Previously, this N terminus of TGase 2 was identified as fibronectin (Hang et al. 2005) or a p53 binding region (Kang et al. 2016) (Fig. 2b). The GK921 binding region was marked with red ribbon in the unfolded form of TGase 2 (Fig. 2b). We have shown that in vitro TGase 2 inhibitory effect of GK921 was IC50: 8.93 μM (Supple Fig. 1a) (Ku et al. 2014). Therefore, GK921 binds to the N terminus of TGase 2 (non-active site) as well as GK921 inhibits TGase 2 activity in vitro. The question remains whether GK921 binding to TGase 2 triggers

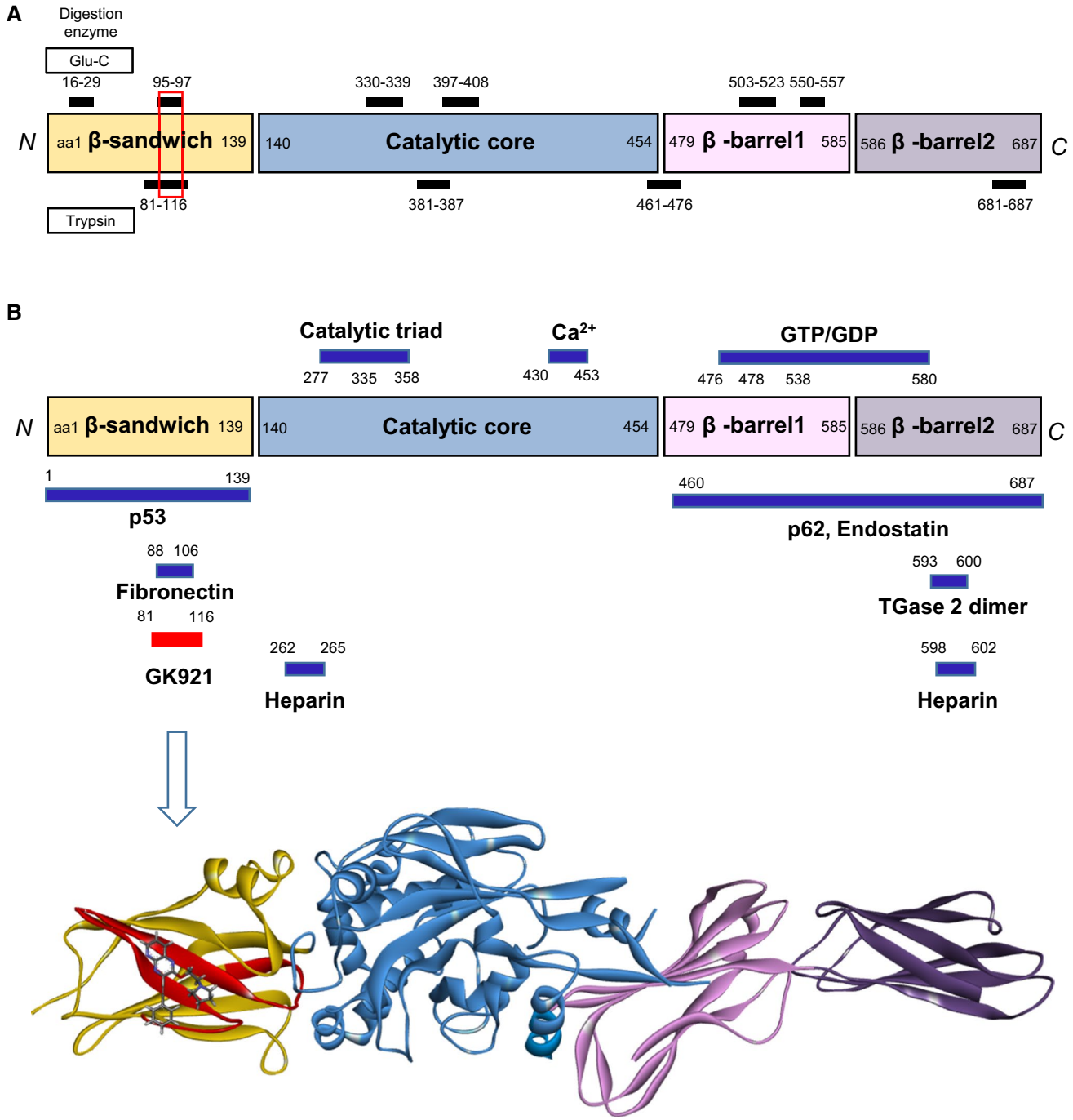

Fig. 2 Identification of binding site of GK921 on purified recombinant human TGase 2. **a** To identify the binding site of GK921 on TGase 2, mass spectrometry analysis was employed following incubation of TGase 2 and GK921 for 30 min at RT. The mass coverage from samples revealed the difference between TGase 2 alone and the combination of TGase 2 and GK921. The GK921 binding-mediated masking region of TGase 2 is denoted by underline 81–116, 381–387, 461–476, and 681–687 in solution trypsin digestion and 16–29, 95–97, 330–339, 397–408, 503–523 and 550–557 in solution Glu-C digestion. The merged GK921 binding-mediated masking region of TGase 2 is 81–116 in solution trypsin and Glu-C digestion although exact masking sequence was 95–97. **b** The four domains of TGase 2 are presented with binding domains. The catalytic core domain of TGase 2 is responsible for its enzymatic activity by Ca^{++} (430–453 a.a). The β-barrel 1 domain of TGase 2 contains heparin binding site (262–265 a.a) (Lortat-Jacob et al. 2012) and a guanosine-tri/di-phosphate (GTP/GDP) binding site (476–478; 538–580 a.a) (Han et al. 2010; Liu et al. 2002; Noguchi et al. 2001). The C-terminal β-barrel 2 domain of TGase 2 contains heparin binding site (598–602 a.a) (Lortat-Jacob et al. 2012) and TGase 2 dimer (593–600 a.a) (Kim et al. 2017). The combined β-barrel 1 and 2 domain of TGase 2 contains p62 (460–687 a.a) (Kang et al. 2016) and endostatin (460–687 a.a) binding site (Faye et al. 2010)

conformational change as an allosteric effect of TGase 2 activity in vitro. Therefore, we have employed native gel PAGE to test whether GK921 induces conformational change in a dose-dependent manner.

GK921 triggered self-polymerization of TGase 2 through conformational change

GK921 induced conformational change of TGase 2 in a dose-dependent manner at 37 °C (Fig. 3a), which is not a covalently changed conformation because SDS PAGE showed no change of molecular weight size. The acceleration of polymerization of TGase 2 has been observed by temperature increase only in the native PAGE (Kim et al. 2017). This conformational change of purified recombinant TGase 2 affects size-exclusion chromatography (Kim et al. 2017). TGase 2 triggers self-dimer formation from a monomeric state under 37 °C which is according to the previous report (Fig. 3a) (Kim et al. 2017). Native gel electrophoresis revealed that TGase 2 incubation with GK921 induced acceleration of self-dimer and self-polymers in a dose-dependent manner under 37 °C (Fig. 3a). In contrast, SDS gel electrophoresis showed no molecular weight change at all (Fig. 3a). This implies that TGase 2 self-polymerization is due to non-covalent interactions, such as hydrophilic or hydrophobic interactions, due to the change of TGase 2 conformation. To test whether GK921 binds proteins specifically, GK921 was incubated with two proteins of lactate dehydrogenase or fibrinogen (Fig. 3b). Two proteins did not show dimer, trimer, polymer formations with GK921 either in the native gel or in SDS gel electrophoresis (Fig. 3b). This implies that GK921 binding on TGase 2 may be specific.

Complex structure modeling of GK921 with TGase 2

From the results of the fluorescence assay (Fig. 1b), mass analysis (Fig. 2a), and a previously published paper (Kang et al. 2016), GK921 binds to the N terminus of TGase 2. To support these results, the GK921 binding site was screened using computational analysis. First, the GK921 binding site was screened for the whole region of TGase 2 (PDB:2Q3Z) using the CDOCKER protocol to run a CHARMm-based molecular dynamics algorithm to dock GK921 into TGase 2 by Discovery studio. Interestingly, it was confirmed that the TGase 2 structure has a GK921 binding site at the N terminus in the several putative binding regions (Fig. 4a). In silico analysis confirmed the possibility that the binding site of GK921 may be present at the N terminus; for this reason, the binding site of GK921 was narrowed to the N terminus region and analyzed. Thus, the binding site of GK921 is displayed on the surface of TGase 2, and GK921 binds to the hydrophobic region of TGase 2 (Fig. 4b). The N-terminal structure of TGase 2 was converted to a solid ribbon model, and mass results of GK921 binding were shown in red. Thus, the result of the mass estimation and the computer analysis of the GK921 binding site showed 83–103 a.a of the N terminus of TGase 2, which concurred with the M/S analysis for the binding region in Fig. 2 (81–116 a.a). The GK921 binding model showed that Val83, Glu85, Val93 and Gln103 of TGase 2 have a critical interaction with building blocks of GK921 (Fig. 4b). From the gel electrophoresis results, the multimerization of TGase 2 is not increased in size irregularly, but it is doubled by dimer, tetramer, etc., regularly (Fig. 3a). This multimerization is thought to occur under normal conditions, but the reaction rate is thought to be increased by GK921 binding. The N-terminal domain of TGase 2 (81–116 a.a) predicted to bind to GK921 was calculated to be a strong aggregation hot spot as a hydrophobic region (Fig. 4c). The aggregation hot spot of the N terminal is covered by GK921 (Fig. 4d). It is observed that the binding of GK921 induces increase of dimerization by conformational changes. Further studies about the multimerization mechanism of TGase 2 by GK921 are needed in the future.

GK921 inhibits p53 binding at N terminus of TGase 2

Previously we have tested whether GK921 directly binds to p53. When we had treated 1 μM of GK921 on HEK293 cells that presented no TGase 2 expression and wild-type p53, we have detected no p53 activity by BAX-luciferase reporter assay (Ku et al. 2014). GK921 has a very efficient anti-cancer effect on renal cell carcinoma by stabilization of p53 in a dose-dependent manner (Ku et al. 2014). The N terminus (1–139 a.a) of TGase 2 is the binding region of p53 (Kang et al. 2016). Therefore, GK921-induced p53 stabilization was an inhibition effect of p53 binding to TGase 2 by competition at p53 binding site of TGase 2. To test whether GK921 competes with p53 for binding to the N terminus of TGase 2, a mixture of TGase 2 and p53 was incubated with GK921 at 37 °C for 30 min in vitro (Fig. 5a). Immunoblotting of TGase 2 after immunoprecipitation of p53 showed that GK921 reduced p53 binding to TGase 2 in a dose-dependent manner (Fig. 5a). To determine whether GK921 has the same effect on cells, ACHN (Fig. 5b) cells and HEK293 transfected with HA-TGase 2 and 3xFLAG-p53 cells (Fig. 5c) were treated with GK921 for 24 h. The result showed that GK921 reduced TGase 2 binding to p53 in a dose-dependent manner (Fig. 5b, c). To confirm the TGase 2 binding site of GK921 at N terminus of TGase 2 in Fig. 4, we constructed TGase 2 quadruple point mutant targeting charged amino acids in the N terminus (Q95A, Q96A, Q103A, R116A) (Fig. 5d). To test whether GK921 binds specifically to N terminus of TGase 2 around 81–116 a.a, HEK293 cells were treated with GK921 after cells were transfected with HA-TGase 2 WT, HA-TGase 2 MT containing point mutations at Q95A, Q96A, Q103A, R116A

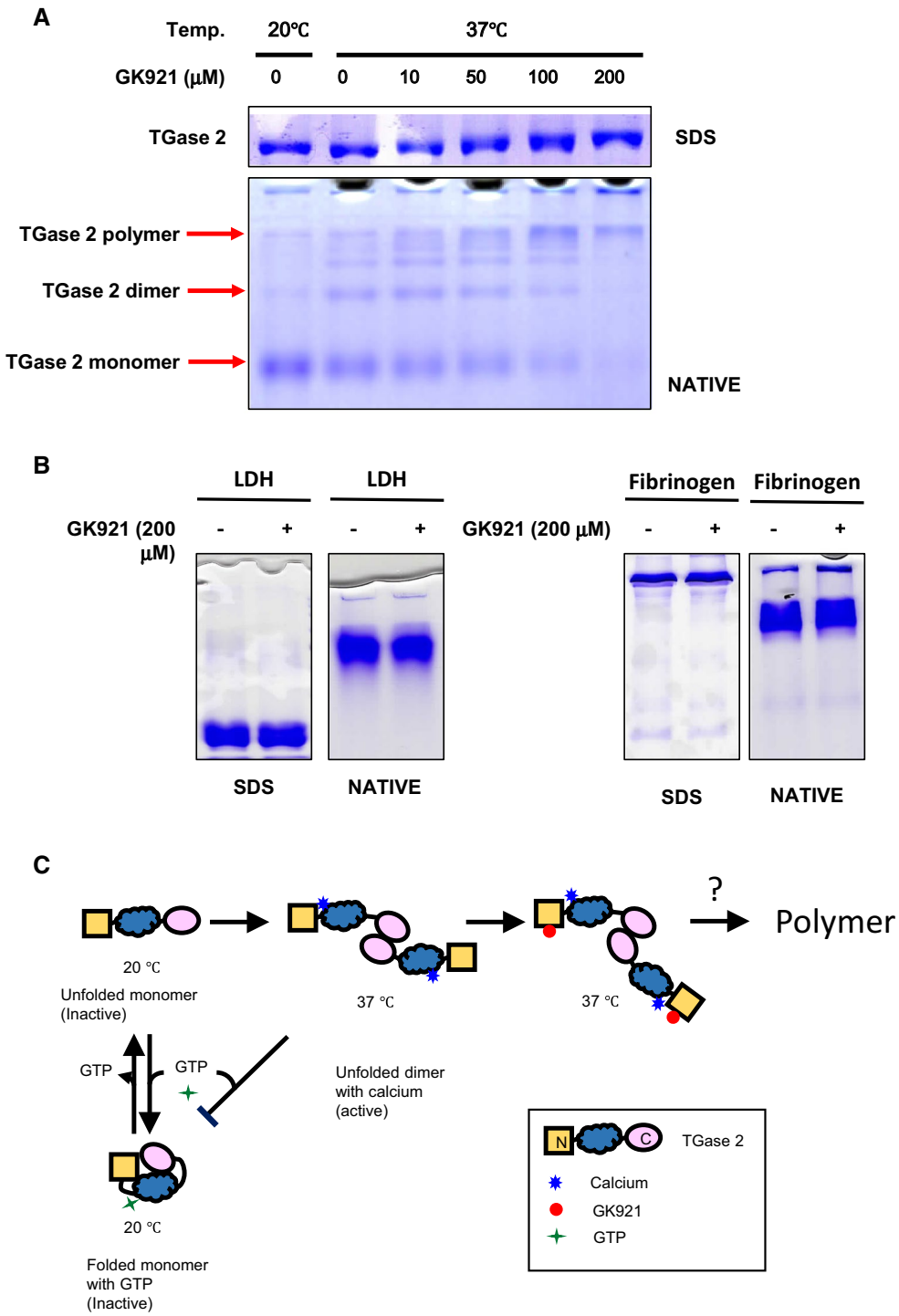

Fig. 3 Conformational change of purified recombinant human TGase 2 by GK921 binding. **a** The conformational change of TGase 2 was observed after incubation with GK921 by native gel. The purified TGase 2 was incubated with GK921, run by native gel, and stained with Coomassie blue. Monomer, dimer, and polymer of TGase 2 were observed at 37 °C without GK921. TGase 2 polymers were increased while TGase 2 monomer was reduced with incubation of GK921 in a dose-dependent manner. Data are representative of three independent experiments. **b** The conformation change of lactate dehydrogenase (LDH) or fibrinogen was not observed after incubation with GK921 by native gel. Data are representative of three independent experiments. **c** A model of TGase 2 dimer activation and inhibition by GK921

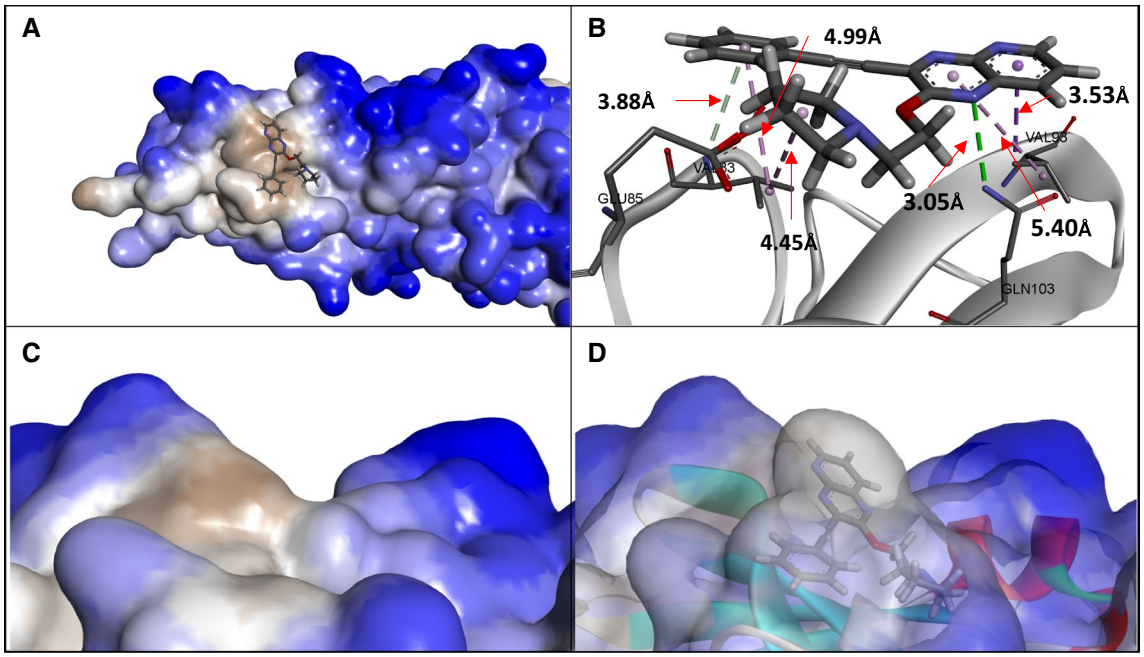

Fig. 4 In silico analysis of GK921 binding site of human TGase 2. **a** The overall structure domain of TGase 2 and GK921 binding site. GK921 docked to between the N-terminal β-sandwich domain of TGase 2. **b** The focused region of TGase 2 and the GK921 binding site. **c** The non-covalent interaction between GK921 and TGase 2. **d** Ligand interaction 2D diagram of GK921 in the TGase 2. Interactions are shown as dashed lines between TGase 2 residues and GK921 atoms. Neighboring residues are colored green; the solvent accessible surface of an interacting residue is represented by a halo around the residue. The diameter of the circle is proportional to the solvent accessible surface

and FLAG-p53, respectively. Co-immunoprecipitation of TGase 2 was performed using anti-HA antibody and p53 binding was detected by immunoblotting with FLAG antibody as described in the methods (Fig. 5e). Wild-type TGase 2 showed 50% reduction of p53 binding while mutant form of TGase 2 showed no reduction of p53 binding at 1 μM of GK921 treatment (Fig. 5e). This confirms that GK921 binds at N terminus of TGase 2 around 81–116 a.a, which induces binding hindrance of TGase 2 to p53.

Discussion

Most TGase 2 inhibitor developers aim at the active site or the GTP binding site of TGase 2 based on X-ray crystal structures (Liu et al. 2002; Han et al. 2010; Pinkas et al. 2007). Recent understanding of the TGase 2 structure involved unfolded (active) or folded (inactive) forms of TGase 2 regulated by calcium and GTP, respectively (Pinkas et al. 2007). The proposed theory was that TGase 2 was in a folded conformation with GTP as an inactive form. Calcium binding to TGase 2 would then release GTP, opening the active site as an active form. Although there is a limit in applying this theory to physiological conditions, because the unfolded form of the TGase 2 crystal was made with TGase 2 inhibitors under 4 °C, and also because the physiological GTP level is not sufficient to maintain TGase 2 in its folded form in every cell compartment, the theory was widely accepted until we found temperature-sensitive conformational change in TGase 2 (Kim et al. 2017). Recently, we found that TGase 2 without GTP is produced as an unfolded monomer under room temperature and undergoes non-covalent dimerization as an unfolded form over 30 °C (Fig. 3) (Kim et al. 2017). Unfolded dimeric TGase 2 is the most stable conformation of the enzyme at 37 °C (Fig. 3a, c) (Kim et al. 2017). Multimeric forms of TGase 2 can be processed through interactions between dimers and tetramers during incubation in vitro at 37 °C, but these are the results of protein–protein interactions without involving covalent crosslinks (Fig. 3a, c) (Kim et al. 2017). This clearly suggests a challenging task for us to re-calculate cross-linking reactions by TGase 2 as an unfolded dimeric form instead of a folded monomeric form. In this study, we found that GK921 binding to TGase 2 induced non-covalent polymerization of TGase 2 (Fig. 3a, c), which might be due to change of TGase 2 surface charge (Fig. 4c, d). This implies that the GK921 binding site of TGase 2 (81–116 a.a) may be an allosteric site for triggering enzymatic conformation change. Interestingly, this GK921 binding site of TGase 2 is shared with the fibronectin binding site (88–106 a.a) (Gaudry et al. 1999). It is easily understood that fibronectin binding to TGase 2 may trigger polymerization through

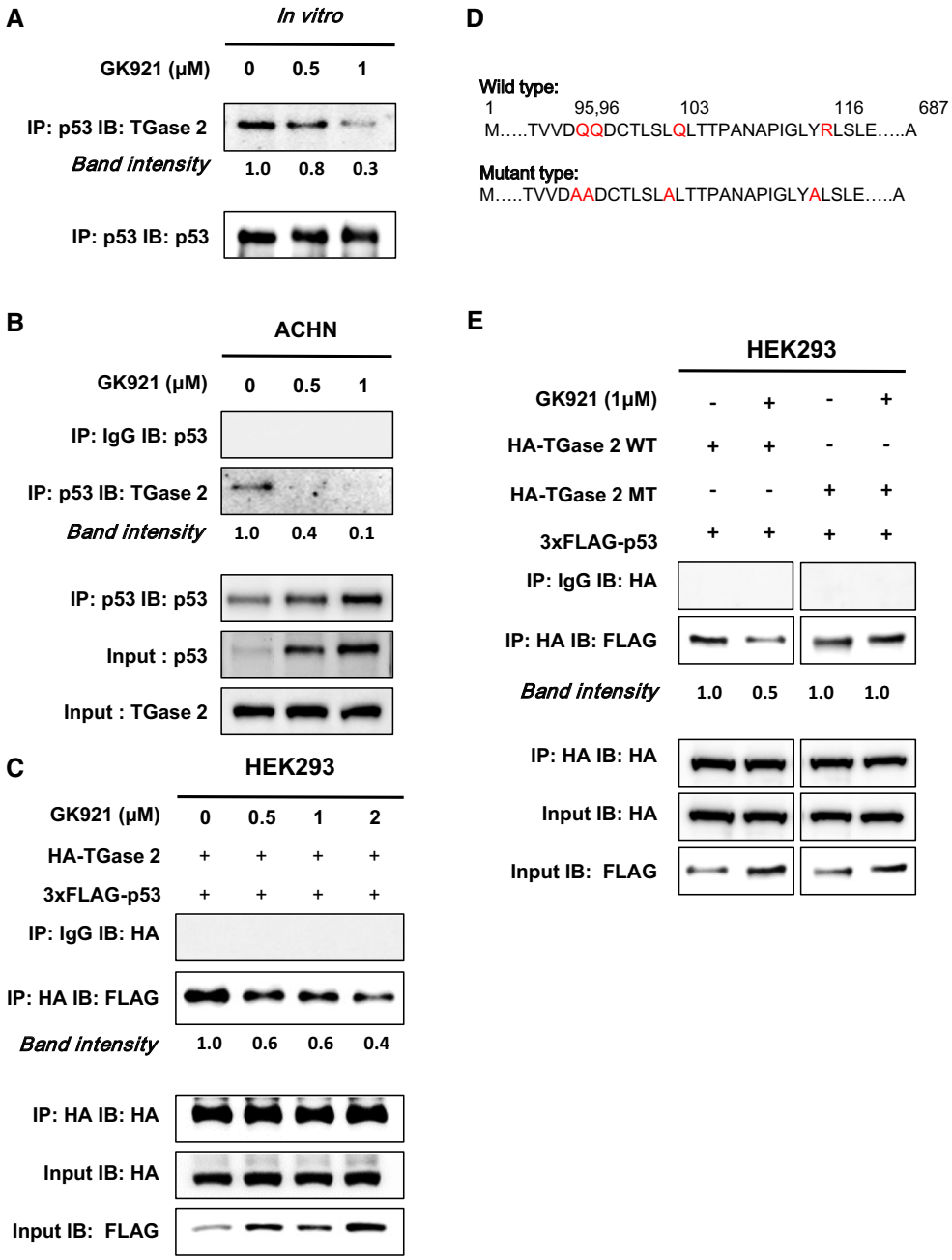

Fig. 5 GK921 inhibits p53 and TGase 2 interaction. **a** To test whether GK921 binding to purified recombinant human TGase 2 competes with purified human recombinant p53 binding to TGase 2 in vitro, co-immunoprecipitation of p53 was performed using p53 antibody and immunoblotting was performed using TGase 2 antibody after incubation of TGase 2 with p53 and GK921 in a dose-dependent manner (0, 0.5, 1 μM). Immunoblots were quantified using densitometry. **b** To test whether GK921 binding to TGase 2 competes with p53 binding to TGase 2 in RCC cell, co-immunoprecipitation was performed using p53 antibody and TGase 2 binding to p53 was detected by immunoblotting with TGase 2 antibody after ACHN cells were treated with GK921. Immunoblots were quantified using densitometry. **c** To test whether GK921 binding to TGase 2 competes with p53 binding to TGase 2 in normal cell, cells were treated with GK921 in a dose-dependent manner after HEK293 cells were transfected with HA-TGase 2 and FLAG-p53 plasmids concomitantly. Co-immunoprecipitation of TGase 2 was performed using anti-HA antibody and p53 binding was detected by immunoblotting with FLAG antibody. Immunoblots were quantified using densitometry. **d** To indentify the TGase 2 binding site of GK921, we constructed TGase 2 quadruple point mutant (Q95A, Q96A, Q103A, R116A). **e** To confirm whether GK921 binds specifically TGase 2 N terminus, HEK293 cells were treated with GK921 after cells were transfected with HA-TGase 2 WT, HA-TGase 2 MT and FLAG-p53, respectively. Co-immunoprecipitation of TGase 2 was performed using anti-HA antibody and p53 binding was detected by immunoblotting with FLAG antibody. Data are representative of three independent experiments

allosteric conformation change for matrix formation or blood coagulation as a substrate (Barsigian et al. 1991).

The mechanism of TGase 2-mediated iso-peptide formation has been elucidated using active site cysteine (C277) (Folk 1983; Folk and Chung 1973). Iso-peptide formation involves three steps, namely the acylation of substrate A, transition of substrate A–enzyme–substrate B, and transamidation between A and B (Keillor et al. 2015). In the acylation state, a catalytic triad was proposed as C277, H335, D358 using a folded form of TGase 2 by Liu et al. (2002). Later, another model was suggested as C277, W241, W332 using an unfolded form of TGase 2 (Pinkas et al. 2007). TGase 2 binds to GDP at S482 and R580 for formation of a folded form Liu et al. (2002). TGase 2 has a cysteine triad around the active site (C277) as C230, C370, C371 (Han et al. 2010), which can be disulfide bonded under oxidation for activity regulation (Stamnaes et al. 2010). Although the crystallographic structure of the open conformation of TGase 2 proposed an acyl-donor substrate binding site (Keillor et al. 2015), it is not enough for two large TGase 2 substrate molecules. Interestingly, TGase 2 establishes an iso-peptide bond between large proteins such as 340 kDa fibrinogen (Kimura and Aoki 1986), 347 kDa huntingtin (Karpuj et al. 1999), 40 kDa I-κBα (Lee et al. 2004), 55 kDa p53 (Ku et al. 2013) and 45 kDa VEGF (vascular endothelial growth factor) (Zisch et al. 2001). Therefore, active TGase 2 in its unfolded conformation is unable to fit between two large proteins due to the small size of the catalytic pocket. This clearly suggests that we need to re-calculate the cross-linking reaction by TGase 2 as an unfolded dimeric form instead of a folded monomeric form. GTP inactivates monomeric TGase 2 as a folded form below room temperature at high concentration. However, TGase 2 activity is likely controlled by the oxidative state instead of GTP binding, because the physiological level of GTP is less than 100 μM. Highly oxidative conditions were reported to keep TGase 2 in the inactive state in the absence of chemical stresses (Siegel et al. 2008) due to the formation of an inhibitory disulfide bond between the residues C370 and C371 (Han et al. 2010; Stamnaes et al. 2010).

In conclusion, GK921 binds at the N terminus of TGase 2 around 81–116 a.a, which induces binding hindrance of TGase 2 to p53. From this mechanism, it can be explained that GK921 has a very efficient anti-cancerous effect on renal cell carcinoma with high expression of TGase 2 by stabilization of p53 in a dose-dependent manner. Furthermore, the N terminus of TGase 2 (81–116 a.a) revealed to control TGase 2 activity as an allosteric binding site, which can trigger conformational change by binding GK921.

Acknowledgments This research was supported by a grant from the National Cancer Center of Korea (NCC1410280-5).

Compliance with ethical standards

Conflict of interest The authors have no conflicts of interest (financial or non-financial) to declare.

Ethical approval Authors make sure that the manuscript complies with the ethical rules applicable for this journal.

References

Barsigian C, Stern AM, Martinez J (1991) Tissue (type II) transglutaminase covalently incorporates itself, fibrinogen, or fibronectin into high molecular weight complexes on the extracellular surface of isolated hepatocytes. Use of 2-[(2-oxopropyl)thio] imidazolium derivatives as cellular transglutaminase inactivators. J Biol Chem 266(33):22501–22509

Faye C, Inforzato A, Bignon M, Hartmann DJ, Muller L, Ballut L, Olsen BR, Day AJ, Ricard-Blum S (2010) Transglutaminase-2: a new endostatin partner in the extracellular matrix of endothelial cells. Biochem J 427(3):467–475. https://doi.org/10.1042/BJ20091594

Folk JE (1983) Mechanism and basis for specificity of transglutaminase-catalyzed epsilon-(gamma-glutamyl) lysine bond formation. Adv Enzymol Relat Areas Mol Biol 54:1–56

Folk JE, Chung SI (1973) Molecular and catalytic properties of transglutaminases. Adv Enzymol Relat Areas Mol Biol 38:109–191

Gaudry CA, Verderio E, Aeschlimann D, Cox A, Smith C, Griffin M (1999) Cell surface localization of tissue transglutaminase is dependent on a fibronectin-binding site in its N-terminal beta-sandwich domain. J Biol Chem 274(43):30707–30714

Han BG, Cho JW, Cho YD, Jeong KC, Kim SY, Lee BI (2010) Crystal structure of human transglutaminase 2 in complex with adenosine triphosphate. Int J Biol Macromol 47(2):190–195. https://doi.org/10.1016/j.ijbiomac.2010.04.023

Hang J, Zemskov EA, Lorand L, Belkin AM (2005) Identification of a novel recognition sequence for fibronectin within the NH2-terminal beta-sandwich domain of tissue transglutaminase. J Biol Chem 280(25):23675–23683. https://doi.org/10.1074/jbc.M503323200

Hidaka H, Seki N, Yoshino H, Yamasaki T, Yamada Y, Nohata N, Fuse M, Nakagawa M, Enokida H (2012) Tumor suppressive microRNA-1285 regulates novel molecular targets: aberrant expression and functional significance in renal cell carcinoma. Oncotarget 3(1):44–57. https://doi.org/10.18632/oncotarget.417

Kang JH, Lee JS, Hong D, Lee SH, Kim N, Lee WK, Sung TW, Gong YD, Kim SY (2016) Renal cell carcinoma escapes death by p53 depletion through transglutaminase 2-chaperoned autophagy. Cell Death Dis 7:e2163. https://doi.org/10.1038/cddis.2016.14

Karpuj MV, Garren H, Slunt H, Price DL, Gusella J, Becher MW, Steinman L (1999) Transglutaminase aggregates huntingtin into nonamyloidogenic polymers, and its enzymatic activity increases in Huntington's disease brain nuclei. Proc Natl Acad Sci U S A 96(13):7388–7393

Keillor JW, Apperley KY, Akbar A (2015) Inhibitors of tissue transglutaminase. Trends Pharmacol Sci 36(1):32–40. https://doi.org/10.1016/j.tips.2014.10.014

Kim N, Lee WK, Lee SH, Jin KS, Kim KH, Lee Y, Song M, Kim SY (2017) Inter-molecular crosslinking activity is engendered by the dimeric form of transglutaminase 2. Amino Acids 49(3):461–471. https://doi.org/10.1007/s00726-016-2293-1

Kimura S, Aoki N (1986) Cross-linking site in fibrinogen for alpha 2-plasmin inhibitor. J Biol Chem 261(33):15591–15595

Ku BM, Kim DS, Kim KH, Yoo BC, Kim SH, Gong YD, Kim SY (2013) Transglutaminase 2 inhibition found to induce p53 mediated apoptosis in renal cell carcinoma. FASEB J 27(9):3487–3495. https://doi.org/10.1096/fj.12-224220

Ku BM, Kim SJ, Kim N, Hong D, Choi YB, Lee SH, Gong YD, Kim SY (2014) Transglutaminase 2 inhibitor abrogates renal cell carcinoma in xenograft models. J Cancer Res Clin Oncol 140(5):757–767. https://doi.org/10.1007/s00432-014-1623-5

Lee J, Kim YS, Choi DH, Bang MS, Han TR, Joh TH, Kim SY (2004) Transglutaminase 2 induces nuclear factor-kappaB activation via a novel pathway in BV-2 microglia. J Biol Chem 279(51):53725–53735. https://doi.org/10.1074/jbc.M407627200

Liu S, Cerione RA, Clardy J (2002) Structural basis for the guanine nucleotide-binding activity of tissue transglutaminase and its regulation of transamidation activity. Proc Natl Acad Sci U S A 99(5):2743–2747. https://doi.org/10.1073/pnas.042454899

Lortat-Jacob H, Burhan I, Scarpellini A, Thomas A, Imberty A, Vives RR, Johnson T, Gutierrez A, Verderio EA (2012) Transglutaminase-2 interaction with heparin: identification of a heparin binding site that regulates cell adhesion to fibronectin-transglutaminase-2 matrix. J Biol Chem 287(22):18005–18017. https://doi.org/10.1074/jbc.M111.337089

Noguchi K, Ishikawa K, Yokoyama K, Ohtsuka T, Nio N, Suzuki E (2001) Crystal structure of red sea bream transglutaminase. J Biol Chem 276(15):12055–12059. https://doi.org/10.1074/jbc.M009862200

Park MJ, Baek HW, Rhee YY, Lee C, Park JW, Kim HW, Moon KC (2015) Transglutaminase 2 expression and its prognostic significance in clear cell renal cell carcinoma. J Pathol Transl Med 49(1):37–43. https://doi.org/10.4132/jptm.2014.10.25

Pinkas DM, Strop P, Brunger AT, Khosla C (2007) Transglutaminase 2 undergoes a large conformational change upon activation. PLoS Biol 5(12):e327. https://doi.org/10.1371/journal.pbio.0050327

Stamnaes J, Pinkas DM, Fleckenstein B, Khosla C, Sollid LM (2010) Redox regulation of transglutaminase 2 activity. J Biol Chem 285(33):25402–25409. https://doi.org/10.1074/jbc.M109.097162

Yin J, Oh YT, Kim JY, Kim SS, Choi E, Kim TH, Hong JH, Chang N, Cho HJ, Sa JK, Kim JC, Kwon HJ, Park S, Lin W, Nakano I, Gwak HS, Yoo H, Lee SH, Lee J, Kim JH, Kim SY, Nam DH, Park MJ, Park JB (2017) Transglutaminase 2 inhibition reverses mesenchymal transdifferentiation of glioma stem cells by regulating C/EBPbeta signaling. Cancer Res. https://doi.org/10.1158/0008-5472.CAN-17-0388

Zisch AH, Schenk U, Schense JC, Sakiyama-Elbert SE, Hubbell JA (2001) Covalently conjugated VEGF–fibrin matrices for endothelialization. J Control Release 72(1–3):101–113